tvst

https://doi.org/10.1167/tvst.7.5.2

Article

Quantification of the Posterior Cornea Using Swept Source Optical Coherence Tomography

Stephen Wahlig[1,2], Gary Hin-Fai Yam[1,3], Wesley Chong[3], Xin-Yi Seah[1], Viridiana Kocaba[1,5,6], Marcus Ang[1,3,4,7], Hla Myint Htoon[1,4], Tin A. Tun[1,3], Hon Shing Ong[1,3,7], and Jodhbir S. Mehta[1,3,4]

[1] Singapore Eye Research Institute (SERI), Singapore
[2] Duke University School of Medicine, Durham, NC, USA
[3] Singapore National Eye Center (SNEC), Singapore
[4] Eye-ACP, Duke-NUS Graduate Medical School, Singapore
[5] Department of Ophthalmology, Edouard Herriot Hospital, Hospices Civils de Lyon, Lyon, France
[6] Université de Lyon, F-69000 Lyon, France; Université Lyon 1, F-69100 Villeurbanne, France
[7] Moorfields Eye Hospital, London, UK

Correspondence: Jodhbir S. Mehta, Singapore Eye Research Institute, 20 College Rd, The Academia Discovery Tower Level 6, Singapore 169856. e-mail: jodmehta@gmail.com

Received: 19 February 2018
Accepted: 15 July 2018
Published: 4 September 2018

Keywords: corneal endothelium; cornea; transition zone; trabecular meshwork

Citation: Wahlig S, Yam GH-F, Chong W, Seah X-Y, Kocaba V, Ang M, Htoon HM, Tun TA, Ong HS, Mehta JS. Quantification of the posterior cornea using swept source optical coherence tomography. Trans Vis Sci Tech. 2018;7(5):2, https://doi.org/10.1167/tvst.7.5.2

Purpose: We define optical coherence tomography (OCT) measurement parameters of the corneal endothelium/Descemet's membrane (DM) complex and peripheral transition zone (TZ) and describe these measurements in an ethnically Chinese population.

Methods: OCT images of the anterior segment and iridocorneal angle were obtained from 129 healthy Chinese subjects (129 eyes), aged 40 to 81 years. The scleral spur (SS) and Schwalbe's line (SL) were identified in each image. Endothelium/DM diameter, referred to as endothelial arc length (EAL), is the SL-to-SL distance. The SS-to-SL distance encompasses the TZ and trabecular meshwork (TM). Since the TZ cannot be visualized by OCT, a ratio of TZ-to-TZ+TM width was calculated from scanning electron microscopy (SEM) images obtained from 5 cadaveric corneas. The SS-to-SL distance was multiplied by this ratio to approximate in vivo TZ width.

Results: From SEM measurements, the relationship TZ = 0.20*(TZ+TM) was determined. From OCT measurements, mean EAL was 12.15 ± 0.58 mm and mean TZ width was 156 ± 20 μm. For eyes with horizontal and vertical images, vertical EAL was significantly greater than horizontal EAL ($P = 0.03$).

Conclusions: Corneal endothelium/DM diameter and TZ width can be obtained from OCT images. Although only combined TZ+TM is visualized on OCT, TZ width can be reasonably approximated.

Translational Relevance: Emerging procedures, like endothelial cell injection and DM transplantation (DMT), require accurate measurements of endothelium/DM size for preoperative planning. Size of the TZ, which may contain progenitor cells, also could contribute to endothelial regeneration in these procedures.

Introduction

The corneal endothelium is a single cell layer that lines the innermost surface of the posterior cornea and regulates corneal hydration.[1] Corneal endothelial dystrophies, infections, inflammation, or traumatic insults can cause the human corneal endothelial cell (HCEnC) density to fall below a critical threshold of 500 to 1000 cells/mm^2, with subsequent corneal edema and blindness.[2,3] Currently, the only therapy for endothelial dysfunction is allogeneic transplantation, using either a full-thickness corneal graft, that is, penetrating keratoplasty (PK), or a partial-thickness endothelial graft, that is, Descemet's stripping automated endothelial keratoplasty (DSAEK) and Descemet's membrane (DM) endothelial keratoplasty

(DMEK).[4–6] However, reported successes of descemetorhexis without endothelial keratoplasty (DWEK) and DM transplantation (DMT) procedures that involve DM removal without endothelial graft transplantation, as well as DM endothelial transfer (DMET) in which a nonadherent endothelial graft is inserted into the anterior chamber, imply that host cells can contribute to native endothelial regeneration.[7–12] Recent identification of potential endothelial progenitor cells, particularly in the peripheral transition zone (TZ), supports the hypothesis that cell migration from the periphery contributes to this spontaneous regeneration.[13,14] For patients with a large diameter endothelium/DM complex, the increased migration distance between the peripheral progenitor cells and central defects could limit the potential regenerative response. However, a larger endothelium/DM complex, containing a greater absolute number of HCEnCs, could decrease the amount of cell spreading needed to cover a central defect and mitigate loss of functional reserve.[15] Due to migration distance and functional reserve, host endothelium/DM size and the amount removed in DMET/DWEK/DMT may influence the regenerative response from these procedures;[12] hence, discrepancies in native host endothelium/DM size might partially explain why DMET/DWEK only achieve satisfactory visual recovery in a subset of patients.[12,16,17] Additionally, cellular therapies, such as intracameral HCEnC injection, are emerging as potential clinical alternatives to corneal transplantation (Ong, et al. *IOVS*. 2017;58:ARVO E-Abstract 1476).[18–20] A portion of the host endothelium must be cleared before injection to facilitate attachment of injected cells to the native DM, and determination of the amount of endothelium to be removed will require knowledge of the endothelium/DM size.[12,21] As such, it would be beneficial to identify an accurate in vivo measurement parameter of the host endothelium/DM complex. Furthermore, to this point the TZ has been characterized only in vitro, via scanning electron microscopy (SEM)[22] or immunostaining.[13,23] The ability to measure this region in vivo would enable clinicians to improve our understanding of TZ functionality.

Measurement of the corneal endothelium requires an understanding of the additional structures located on the posterior cornea (Fig. 1). The posterior corneal surface, from center to periphery, consists of the following regions: (1) central endothelium; (2) peripheral endothelium, including a 0.2-mm wide region termed the extreme peripheral endothelium;[23] (3) Schwalbe's line (SL), defined as the terminal edge of the endothelium and DM; (4) transition zone, also known as the smooth zone or Zone S, previously defined as a smooth region without endothelium or trabecular meshwork (TM) fibers;[22,24,25] (5) TM; and (6) the scleral spur (SS), a scleral protrusion in the anterior chamber. Of note, the TZ sometimes is referenced in the literature as Schwalbe's line; we define Schwalbe's line only as the DM edge, while the adjacent 40 to 200 μm region is the TZ.[22,23]

High resolution posterior corneal surface measurements can be achieved using anterior segment optical coherence tomography(AS-OCT)[26] in combination with iridocorneal angle visualization using swept source OCT (SS-OCT).[27,28] Prior studies have quantified the posterior cornea using the posterior corneal arc length (PCAL) parameter, defined as the distance between scleral spurs.[26,29,30] Since this measure includes the TZ and TM width as described above, PCAL overestimates endothelium/DM size. Additionally, quantification of the TM often defines TM width as the distance from SS to SL,[27,31,32] a measure that also includes TZ width. As such, we propose modifying posterior corneal OCT measurements by splitting the SS-to-SL distance into TZ and TM terms, while quantifying endothelium/DM size with the new parameter endothelial arc length (EAL), defined as the SL-to-SL distance. Since the TZ alone cannot be visualized using current OCT technology, in this study we used SEM images taken from five corneoscleral rims to define a ratio of TZ-to-TZ+TM width, which in turn can be used with SS-to-SL measurements to approximate in vivo TZ width. Our aim was to describe these measurements of TZ and EAL in a sample of Chinese subjects and investigate structural factors influencing these parameters.

Methods

Corneoscleral Rim Imaging

All research-grade human cadaver corneal tissues, procured for this study through Lions Eye Institute for Transplant (Tampa, FL) and Research and Miracles in Sight (Winston-Salem, NC), were obtained with informed consent from the next of kin of all deceased donors regarding eye donation for research, and adhered to the principles outlined in the Declaration of Helsinki. A total of five pairs of donor corneal tissues ranging from 51 to 62 years old were procured. Corneoscleral tissues were preserved in Optisol-GS (Bausch & Lomb, Rochester, NY) at

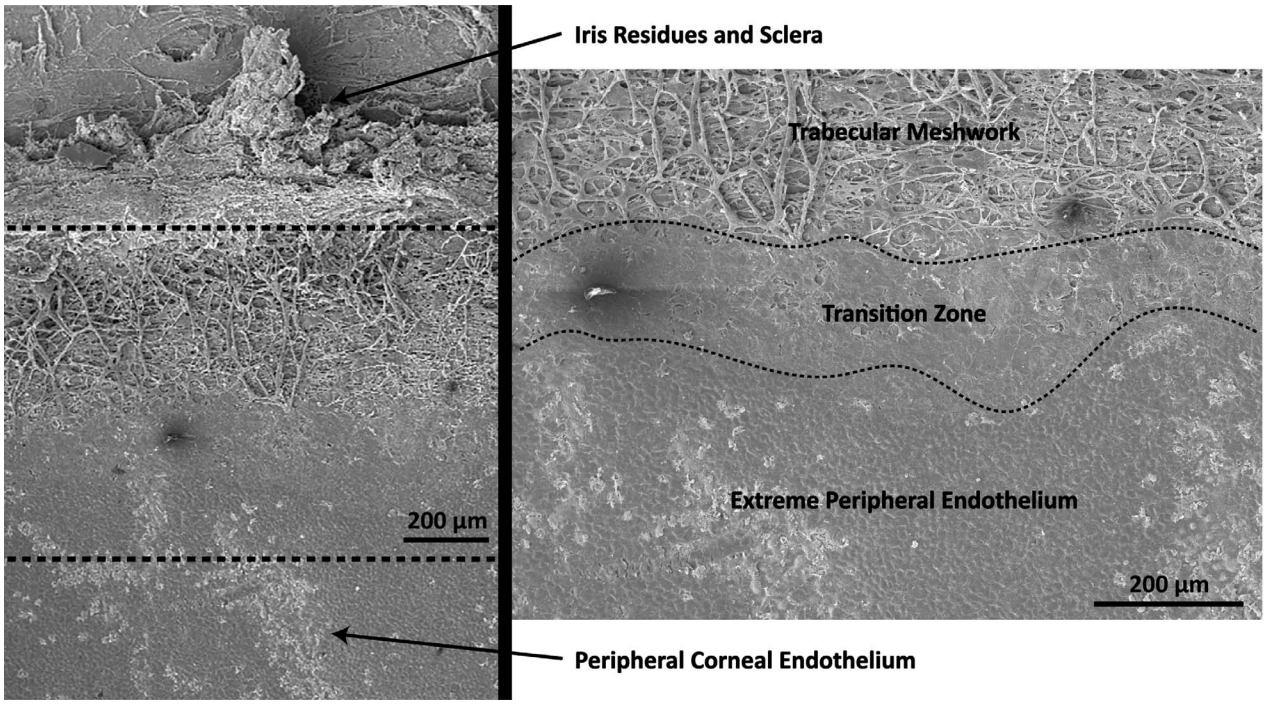

Figure 1. SEM images depicting the structures of interest in the peripheral posterior cornea. The TZ is a relatively smooth area bounded by uveal bands of the TM and polygonal cells of the corneal endothelium.

4°C until they were processed, usually within 14 days of preservation.

Corneas were prepared for SEM as described previously.[33] Briefly, corneoscleral rims were fixed in neutral buffered 2% glutaraldehyde (Electron Microscopy Sciences, Hatfield, PA) at 4°C for 4 hours. After rinses, they were cut into segments and postfixed in aqueous solution of 1% osmium tetroxide at room temperature for 1 hour. The samples were dehydrated under an increasing alcohol gradient, critical point dried (BALTEC, Balzer, Liechtenstein) and mounted onto a metal stub using carbon adhesive tabs. Samples then were sputter-coated for 160 seconds with a 22-nm layer of gold-palladium alloy (BALTEC), and examined under a scanning electron microscope (Quanta 650FEG; FEI, Hillsboro, OR).

SEM Image Analysis

For each segment of corneoscleral rim, image analysis involved manual tracing of the TM area and TZ area using ImageJ (National Institutes of Health, Bethesda, MD). The TZ was defined anteriorly by the border of polygonal endothelium and posteriorly by the uveal bands of the TM (Fig. 1). The TM was defined posteriorly by a raised portion of sclera and anteriorly by the smooth TZ. For multiple sections within each cut segment, an arc length was measured from a curve drawn between the TM and TZ. The TZ and TM width for each section was determined by dividing each respective area by the arc length (Fig. 2). Measurements were conducted by a single examiner (SW). Intraobserver measurement reproducibility was assessed using a subset of three corneas. Width values were averaged to create a single mean TM and TZ width data point for each cut segment. The TZ:(TZ+TM) width ratio used to approximate in vivo TZ width was determined from a linear regression analysis of these data points.

OCT Data Acquisition

The SS-OCT (CASIA SS-1000; Tomey Corporation, Nagoya, Japan) images were obtained from a prior study performed by Tun et al.[27] The study had the approval of the institutional review board of the Singapore Eye Research Institute (CIRB# 2010/297/A), and adhered to the tenets of the Declaration of Helsinki. Written informed consent was obtained from all subjects. Briefly, of 160 subjects recruited from clinics at Singapore National Eye Centre, 19 were excluded from the original study due to incomplete/poor quality imaging SS-OCT data or non-Chinese ethnicity. From the remaining 141 subjects, an additional 12 were excluded from our study for incomplete AS-OCT image data, such that

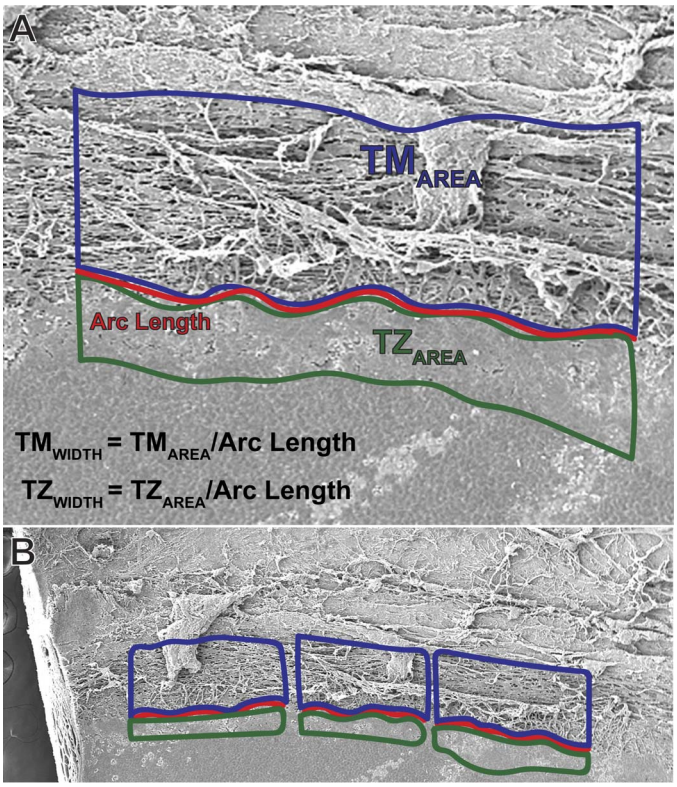

Figure 2. Measurement technique for TZ and TM width. (**A**) TM and TZ areas were traced in ImageJ, and widths were calculated by dividing the areas by the arc length. (**B**) All width values measured within each cut segment were averaged to generate a single data point.

129 eyes were included in the final analysis. All subjects underwent a standardized examination, including measurement of visual acuity, anterior segment evaluation with AS-OCT (Visante; Carl Zeiss Meditec, Dublin, CA), slit-lamp biomicroscopy, and Goldmann applanation tonometry. In addition to standard anterior segment OCT, one randomly selected eye was imaged with the three-dimensional (3D)-angle high definition scan protocol of the SS-OCT to obtain sufficiently high resolution images to identify SL and SS.

A customized software based on ImageJ (Anterior Segment Analysis Program [ASAP]) was used to assess iridocorneal angle structures from the high definition SS-OCT images. After the observer marked the location of the scleral spur and Schwalbe's line, ASAP automatically measured the SS-to-SL distance (Fig. 3). The Zhongshan Assessment Program (ZAP) was used as described previously[30] to analyze the AS-OCT images for determination of central corneal thickness (CCT), anterior chamber depth (ACD), anterior and posterior corneal curvatures (ACC and PCC), and PCAL. The parameters are defined as such: PCAL is the posterior corneal arc distance between scleral spurs, ACC and PCC are the radius of curvature of the anterior and posterior corneal surfaces, respectively. CCT is the perpendicular distance between the anterior and posterior central corneal surfaces, and ACD is the distance from the vertex of the posterior corneal surface to the anterior surface of the crystalline lens (Fig. 3).[26]

Parameter Calculations

TZ+TM width was defined as the SS-to-SL distance, previously described as solely TM width.[27] EAL was defined as the SL-to-SL distance, and calculated by subtracting the TZ+TM width from PCAL. Nasal and temporal TZ+TM values were subtracted from horizontal PCALs, and similarly, superior and inferior TZ+TM were subtracted from vertical PCALs. Since the TZ cannot be directly visualized from the OCT images, TZ width was approximated by multiplying the SS-to-SL distance by the TZ:(TZ+TM) width ratio, as determined from our SEM analysis.

Statistical Analysis

Continuous variables were described as mean and standard deviation (SD). Intraobserver reproducibility for in vitro TZ and TM width measurement was assessed using Bland-Altman analysis. We used simple linear regression to determine the width ratio between in vitro TZ and TZ+TM, and multiple linear regression to assess the relationship of EAL with age, sex, intraocular pressure, and anterior chamber parameters (ACD, PCC, ACC, and CCT). Variance inflation factor (VIF) was calculated to assess for potential multicollinearity among the independent variables. Residual plots of the multiple regression models were examined to assess for normality and constant variance. Adjusted R^2 was calculated to evaluate adequacy of multiple regression models. After checking for normality assumptions of the continuous variables via histogram inspection and Shapiro-Wilk tests, we used a paired sample 2-tailed *t*-test to compare vertical and horizontal EAL within the same eye. $P < 0.05$ was considered statistically significant. All statistical analyses were performed using the R software package (R version 3.4.2, R Foundation for Statistical Computing, Vienna, Austria) and Excel software (Microsoft Corp., Redmond, WA).

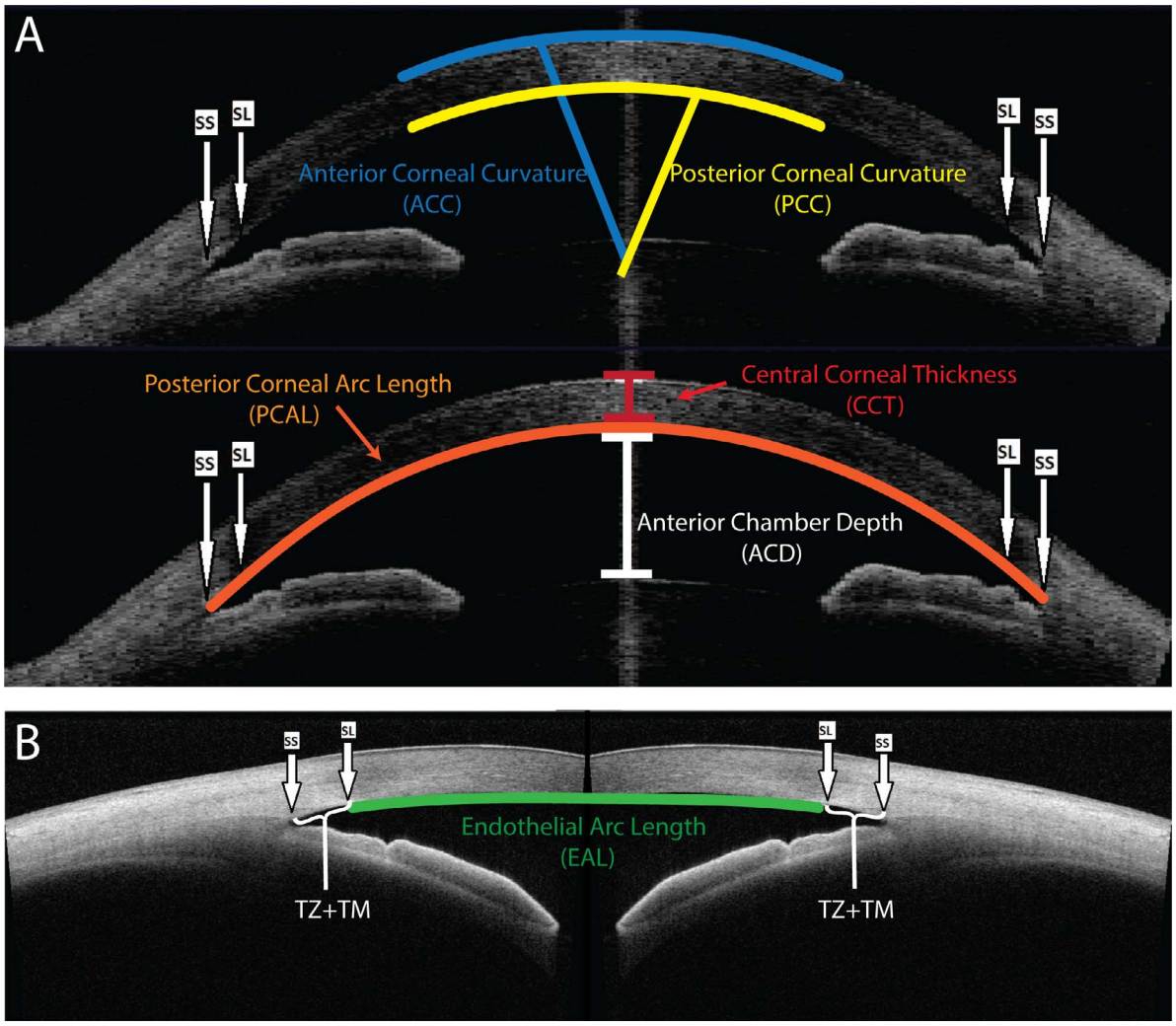

Figure 3. Corneal measurements obtained from OCT images. (**A**) ACC, PCC, PCAL, CCT, and ACD were measured automatically from AS-OCT images using the Zhongshan Assessment Program. (**B**) The TZ+TM distance was measured on high resolution SS-OCT images, and EAL was calculated by subtracting the TZ+TM distance from the PCAL. A user must manually identify the SS and SL in each image.

Results

TZ/TM Analysis

A total of five corneoscleral rims, divided into 36 segments, were analyzed. An annotated version of the corneoscleral rim, illustrating the relevant peripheral corneal structures, is depicted in Figure 1. Mean TZ, TM, and TZ+TM widths were 135 ± 46 (range, 83–269), 548 ± 110 (range, 367–776), and 683 ± 138 (range, 490–999) μm, respectively. Mean differences for intraobserver reproducibility for TZ and TM widths were 2.1 (−21.6, 25.8; 95% confidence interval [CI] limits of agreement) and 0.4 (−33.0, 33.8, 95% CI limits of agreement), μm, respectively. Linear regression analysis of these data yielded the equation TZ = 0.20*(TZ + TM) (R^2 = 0.49), which was used to calculate in vivo TZ width from OCT SL to SS distances (Fig. 4).

OCT Analysis

Of the 129 subjects analyzed, average age was 59.3 ± 9.1 years (range, 40–81) and 64% (82/129) were female. Figure 3 depicts an example measurement of EAL and the TZ+TM width on OCT images. Mean anterior chamber parameters for horizontal and vertical AS-OCT images are detailed in Table 1.

Overall mean EAL was 12.15 ± 0.58 mm (range, 9.91–13.54). Horizontal and vertical EALs were 12.14 ± 0.53 (range, 10.86–13.35) and 12.19 ± 0.73 (range, 9.91–13.55) mm, respectively (Table 2). For the subset of 41 eyes with horizontal and vertical measurements

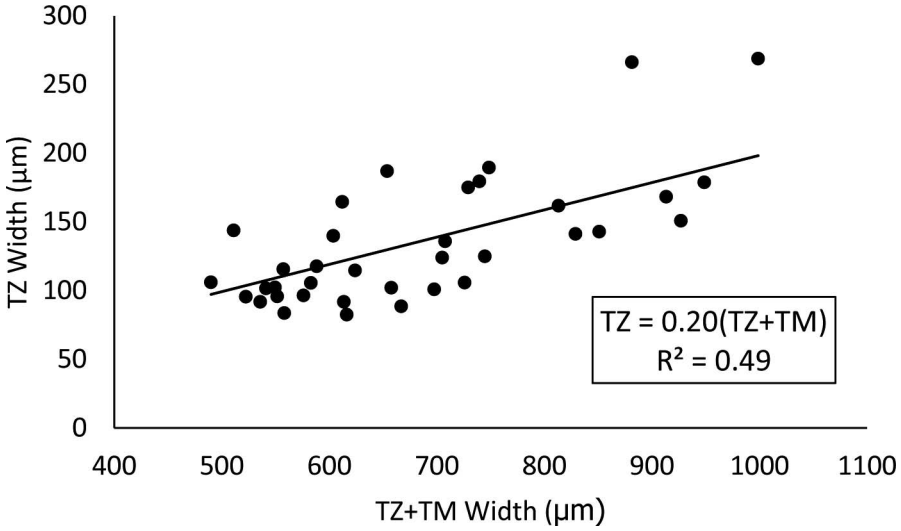

Figure 4. Approximation of TZ width from the combined TZ and TM width. Using measurements from SEM images of cadaveric corneas, TZ width is approximately 20% of combined TZ+TM width. This can be applied to in vivo OCT images, since the scleral spur to Schwalbes' line length is equivalent to TZ+TM.

in the same eye, vertical EALs (12.19 ± 0.74 mm; range, 9.91–13.55) were significantly longer compared to horizontal EALs (12.01 ± 0.52 mm, $P = 0.03$; range, 10.86–13.08). Using multiple linear regression, we determined that ACD, PCC, and ACC are significant determinants of horizontal and vertical EAL (Tables 3, 4). The distribution of residuals followed the normality assumption, and errors

Table 1. ZAP Measurements of Anterior Chamber Parameters

		Corneal Parameters				
Characteristics	*n*	PCAL mm, Mean ± SD	PCC mm, Mean ± SD	CCT µm, Mean ± SD	ACD mm, Mean ± SD	ACC mm, Mean ± SD
Horizontal						
All persons	128	13.59 ± 0.52	6.45 ± 0.35	569.90 ± 34.98	2.59 ± 0.42	7.17 ± 0.42
Age						
40–49	24	13.32 ± 0.54	6.55 ± 0.32	565.83 ± 33.87	2.86 ± 0.37	7.32 ± 0.41
50–59	45	13.72 ± 0.48	6.45 ± 0.39	575.96 ± 31.33	2.60 ± 0.39	7.16 ± 0.47
60–69	43	13.54 ± 0.52	6.40 ± 0.30	565.34 ± 35.35	2.53 ± 0.42	7.09 ± 0.30
≥70	16	13.75 ± 0.41	6.46 ± 0.42	571.04 ± 44.97	2.31 ± 0.35	7.22 ± 0.53
Sex						
Male	47	13.63 ± 0.50	6.48 ± 0.33	569.87 ± 34.30	2.54 ± 0.43	7.21 ± 0.32
Female	81	13.56 ± 0.52	6.44 ± 0.36	569.88 ± 35.58	2.62 ± 0.41	7.15 ± 0.47
Vertical						
All persons	42	13.83 ± 0.77	6.31 ± 0.26	563.67 ± 37.30	2.55 ± 0.54	7.25 ± 0.38
Age						
40–49	5	14.60 ± 0.60	6.36 ± 0.27	542.24 ± 47.77	3.25 ± 0.35	7.23 ± 0.35
50–59	8	13.92 ± 0.54	6.21 ± 0.24	587.86 ± 31.77	2.60 ± 0.53	7.22 ± 0.42
60–69	19	13.76 ± 0.80	6.34 ± 0.29	554.69 ± 34.44	2.50 ± 0.52	7.29 ± 0.45
≥70	10	13.50 ± 0.74	6.31 ± 0.21	572.08 ± 33.83	2.25 ± 0.38	7.19 ± 0.25
Sex						
Male	24	13.92 ± 0.77	6.38 ± 0.28	562.73 ± 31.24	2.52 ± 0.52	7.33 ± 0.33
Female	18	13.71 ± 0.77	6.22 ± 0.20	564.92 ± 45.09	2.59 ± 0.57	7.13 ± 0.44

Table 2. EAL Measurements

Characteristics	*n*	Mean (mm) ± SD
Horizontal		
All persons	128	12.14 ± 0.53
Age		
40–49	24	12.12 ± 0.59
50–59	45	12.21 ± 0.51
60–69	43	12.13 ± 0.49
≥70	16	12.05 ± 0.63
Sex		
Male	47	12.18 ± 0.49
Female	81	12.12 ± 0.55
Vertical		
All persons	42	12.19 ± 0.73
Age		
40–49	5	12.90 ± 0.60
50–59	8	12.22 ± 0.56
60–69	19	12.10 ± 0.80
≥70	10	11.97 ± 0.63
Sex		
Male	24	12.20 ± 0.75
Female	18	12.16 ± 0.72

displayed constant variance upon inspection of the residual versus predicted values plot. For horizontal and vertical EAL, the most important variables were ACD ($\beta = 0.66$, $P < 0.001$ and $\beta = 0.94$, $P < 0.001$, respectively) and PCC ($\beta = 0.70$, $P < 0.001$ and $\beta = 1.48$, $P = 0.004$, respectively). No significant multicollinearity (VIF < 5) was observed (Tables 3, 4). From these models we were able to explain 34.8% of horizontal and 64.1% of vertical EAL variability based on adjusted R^2 values.

Mean SS-to-SL distance was 781 ± 98 μm and mean TZ width, calculated using the TZ:(TZ+TM) ratio of 0.20, was 156 ± 20 μm. TZ width in the superior and inferior quadrants was 158 ± 27 and 178 ± 28 μm, respectively, while the nasal and temporal quadrant widths were 143 ± 27 and 145 ± 24 μm, respectively.

Discussion

Endothelial Arc Length

Using OCT images from a sample of healthy Chinese subjects, we found the average EAL to be 12.15 ± 0.58 mm (range, 9.91–13.54), with vertical EAL values significantly greater than horizontal EAL values in the same eye. This is unexpected, as the horizontal distance typically is greater than vertical distance for conventional anterior corneal measurements.[34] Horizontal and vertical EAL demonstrated a significant correlation with ACD, PCC, and ACC, which is consistent with prior reports of ACD and PCC as determinants of PCAL.[26] Despite these identified predictor parameters, there remains significant unexplained variability in horizontal (adjusted $R^2 = 0.348$) and vertical (adjusted $R^2 = 0.641$) EAL, which may be clarified through future studies using additional anterior chamber parameters and patient data. Furthermore, this is a small sample of 129 eyes, so larger population-based studies will be necessary to validate these trends. Differences in EAL between ethnic groups also should be investigated, as ethnicity has been reported previously to contribute to variability in PCAL, PCC, and anterior chamber area.[26,35]

Knowledge of endothelium/DM size may be useful for optimization of emerging therapies, such as DMET/DWEK/DMT and cellular injection. It remains unclear why DMET and DWEK only stimulate endothelial regeneration and corneal clearance in certain patients.[9,12,16,17] However, DMET has been

Table 3. Multiple Linear Regression Analysis of Horizontal EAL

Variable	Regression Coefficient (β)	95% CI	*P* Value	VIF
ACD (mm)	0.66	(0.46, 0.86)	<0.001*	1.2
PCC (mm)	0.70	(0.36, 1.04)	<0.001*	2.5
ACC (mm)	−0.36	(−0.64, −0.08)	0.014*	2.5
CCT (μm)	0.00	(−0.002, 0.003)	0.973	1.1
Female sex	−0.07	(−0.23, 0.09)	0.381	1.0
Age (yrs)	0.01	(0.00, 0.02)	0.062	1.3
IOP (mm Hg)	0.00	(−0.03, 0.03)	0.901	1.1

IOP, intraocular pressure.
* $P < 0.05$.

Table 4. Multiple Linear Regression Analysis of Vertical EAL

Variable	Regression Coefficient (β)	95% CI	*P* Value	VIF
ACD (mm)	0.94	(0.61, 1.28)	<0.001*	1.7
PCC (mm)	1.48	(0.52, 2.43)	0.004*	3.1
ACC (mm)	−0.66	(−1.31, −0.01)	0.046*	3.2
CCT (μm)	0.00	(−0.004, 0.003)	0.837	1.1
Female sex	0.00	(−0.28, 0.29)	0.979	1.1
Age (yrs)	0.00	(−0.02, 0.02)	0.977	1.4
IOP (mm Hg)	0.00	(−0.05, 0.05)	0.849	1.1

* $P < 0.05$.

reported to produce corneal clearance at a greater rate in patients with Fuchs endothelial corneal dystrophy (FECD) than those with bullous keratopathy.[16] It may be that diffuse endothelial damage in bullous keratopathy injures the peripheral HCEnCs, which would normally stimulate a regenerative response, while this peripheral region is spared in FECD.[12,36] As such, individuals with a larger EAL may possess a greater number of peripheral HCEnCs, which in turn stimulate regeneration of the corneal endothelium after DMET/DWEK/DMT. With preoperative knowledge of a patient's endothelium/DM complex size, clinicians could tailor the size and shape of the DMET/DWEK/DMT descemetorhexis to preserve a consistent amount of peripheral HCEnCs. For example, if a patient has a significantly larger vertical EAL, an oval descemetorhexis with an elongated vertical axis and shortened horizontal axis would be used. This approach would preserve HCEnCs along the smaller endothelial/DM axis, hopefully preventing exhaustion of the regenerative response. Similarly, quadrants with a larger TZ may be able to provide more progenitor cells for endothelial regeneration. An analogous situation exists with therapeutic HCEnC injection, which will require removal of central endothelium using a scraping technique to make room on the host DM for injected cells.[21] Studies of cell injection in felines have shown that scraping a larger segment of host endothelium is correlated with significantly worse outcomes, while eyes with smaller scraped areas demonstrated recovery even without injection of cells.[37] Similar to DMET/DWEK/DMT, eyes with a larger EAL may possess more HCEnCs capable of stimulating regeneration at the edges of the scraped endothelial wound; therefore, host EAL may influence the optimal amount of endothelium to be removed. Determination of the optimal endothelial scraping area would be of significant clinical interest, as excessive removal of host endothelium would require an increase in the number of injected cells and might dampen any native regenerative response, while removal of too little endothelium could prevent adhesion of sufficient exogenous HCEnCs.[12] Furthermore, the variability in native endothelium/DM complex diameter could explain why the critical threshold for HCEnC density spans a wide range from 500 to 1000 cells/mm^2.[2,3,38] Individuals with a larger endothelium/DM diameter may have excess reserve pump functionality that permits a lower HCEnC density before corneal edema occurs. Further clinical investigation is required to investigate each of these hypotheses.

Currently, host endothelium/DM size is determined using white-to-white diameter[29] or PCAL.[26] These parameters can lead to overestimation, while EAL yields an improved measurement by eliminating contributions from iridocorneal angle structures. Additionally, endothelial arc length determination from OCT data requires only user identification of Schwalbe's line and the scleral spur, both of which usually are visible in >95% images with current OCT technology.[26,27]

TZ Width

Using SEM images of cadaveric corneoscleral rims, we were able to identify and measure the TZ and TM. Since only the combined TM and TZ can be visualized from OCT images, it was necessary to use these in vitro data to develop a ratio between TZ and TZ+TM width. From an in vitro TZ width of 135 ± 46 μm and a TM width of 548 ± 110 μm, we arrived at a TZ:(TZ+TM) width ratio of 0.20 (Fig. 4). Applying this equation to the TZ+TM OCT measurements yielded a mean in vivo TZ width of 156 ± 20 μm. Our approximation of in vivo TZ width operates under the assumption that the TZ is located just peripheral to SL as seen in OCT images. This assumption is supported by prior work by Breazzano

et al.[22] in which a suture was placed near Schwalbe's line under OCT guidance and later examined with SEM to confirm localization in the TZ. Our in vitro and in vivo TZ width measurements are slightly elevated compared to prior measurements of 50 – 150 μm,[39] 80-130 μm,[24] and 79 ± 22 μm.[22] However, our in vitro mean TZ+TM width of 683 ± 138 μm is similar to our in vivo SS-to-SL distance of 781 ± 98 μm as well as previously reported SS-to-SL distances of 670 ± 130,[40] 732 ± 27, and 812 ± 13 μm.[31] Of note, ethnicity has not been reported in the earlier in vitro TZ studies; the observed differences in reported values could be a result of ethnic variation. In addition, the study by Breazzano et al.[22] demonstrated significant variability between eyes and between quadrants in the same eye; widths ranged from <40 to >200 μm. This variability underlies the potential clinical u of in vivo TZ quantification; given that the TZ is thought to harbor endothelial progenitor cells,[13,25] a larger TZ could be associated with enhanced endothelial regeneration and an elevated functional reserve in the setting of endothelial dysfunction.

Interestingly, prior studies have indicated TZ width is greatest and least in the superior and inferior quadrants respectively,[22] while TZ+TM width is greatest and least in the inferior and nasal quadrants respectively.[27] Despite our assumptions in approximating TZ width from OCT data, this likely indicates that the TZ:(TZ+TM) width ratio is not fixed throughout the cornea. However, since the TZ study was performed on corneas received from the United States,[22] while the TZ+TM measurements were obtained from an ethnic Chinese population,[27] this difference may partially be a result of ethnic variation. Our data and the earlier TZ SEM publication[22] show that combined superior/inferior TZ width is greater than nasal/temporal width. This orientation might provide UV protection via the eyelids, similar to corneal limbal epithelial stem cells which also are most abundant in the superior and inferior limbus.[41,42] Furthermore, since we have determined that vertical EAL is greater than horizontal EAL, the enlarged vertical TZ segments may reflect the need for a larger progenitor population to migrate across a greater endothelial distance. This finding could hold particular importance with regard to placement of intraocular shunts used to treat glaucoma; while shunt tubes and minimally invasive glaucoma surgery (MIGS) devices are inserted commonly into the superior quadrant,[43,44] such an approach may damage the large superior TZ. Ideally, future refinements of our TZ approximation method could identify the quadrant with the largest ratio of TM-to-TZ width, providing surgeons with maximal room for device insertion while minimizing risk of endothelial progenitor cell damage.

Since this study aimed only to show that it is possible to approximate in vivo TZ width, it has several limitations. As mentioned above, although we used a single TZ:(TZ+TM) ratio to approximate TZ width from OCT measurements, this ratio is likely different within each quadrant. Future determination of TZ:(TZ+TM) width ratios in each quadrant using directionally-oriented corneoscleral rims will be necessary to refine our in vivo TZ approximation technique. Furthermore, logistical constraints necessitated that we derive our TZ:(TZ+TM) width ratio from United States donor corneas rather than Chinese donors to match our in vivo population. Although no information on ethnic differences in TZ has been reported, TM width and several other corneal parameters have been shown to vary between ethnic groups,[26,32,35] indicating that these data from United States corneas may not apply to Chinese subjects. While our primary goal for this study was to demonstrate that our approximation technique yields in vivo TZ width data that is comparable to previously reported in vitro results, future studies will require ethnicity-matched donor corneas and OCT subjects to determine whether TZ width varies with ethnicity. Additionally, SEM analysis using a larger sample size of cadaveric corneas will be necessary to validate the TZ:(TZ+TM) width ratio from this initial study. Ultimately, our indirect approximation technique is inferior to direct in vivo measurement of the TZ. Processing of the corneal samples, including dissection of the rims into segments and chemical fixation, could potentially alter the relevant microanatomy. Cellular boundary retraction in response to SEM processing has been described previously,[45] and may result in underestimation of the cellular TZ width compared to the collagenous TM. However, with the resolution of current OCT images, the TZ borders cannot be directly identified in vivo. In the future, development of ultrahigh-resolution 'micro-OCT,' which is capable of distinguishing individual endothelial cells,[46] may allow for TZ measurement without the need for approximation. Alternatively, wide-field specular microscopy has demonstrated the ability to acquire high resolution images of the corneal periphery.[47,48] However, since it is unclear if wide-field specular microscopy can feasibly acquire images peripheral to

Schwalbes' line, and micro-OCT has not been adapted for human use in vivo, our TZ approximation method is the best available technique to facilitate a larger scale clinical study that will be necessary to investigate potential correlations between the TZ size and endothelial regeneration.

In conclusion, we applied simple manipulations to existing anterior segment OCT measurements to measure the corneal endothelium/DM and peripherally-located TZ. Endothelial/DM complex size, as determined by EAL, was correlated with anterior chamber depth as well as anterior and posterior corneal curvature. Preoperative determination of a patient's EAL may assist clinicians in optimization of DM/endothelium removal as part of emerging procedures, such as DMT/DWEK and intracameral cell injection. As our understanding of peripheral endothelial progenitor cells advances, measurements of TZ width also may gain clinical relevance. Future studies, using a larger number of corneoscleral rims that are ethnically matched and directionally oriented will be necessary to refine this approach.

Acknowledgments

The authors thank Lions Eye Institute for Transplant and Research (Tampa, FL) for their assistance with procurement of research grade donor corneas, and the staff of the Electron Microscopy Unit, National University of Singapore Yong Loo Lin School of Medicine and Experimental Microscopy Supporting Platform, Singapore Eye Research Institute, for assistance with SEM.

Supported by the Singapore National Research Foundation under its Translational and Clinical Research (TCR) program (NMRC/TCR/008-SERI/2013).

Disclosure: **S. Wahlig**, None; **G. Hin-Fai Yam**, None; **W. Chong**, None; **X.-Y. Seah**, None; **V. Kocaba**, None; **M. Ang**, None; **H.M. Htoon**, None; **T.A. Tun**, None; **H.S. Ong**, None; **J.S. Mehta**, None

References

1. Bonanno JA. Molecular mechanisms underlying the corneal endothelial pump. *Exp Eye Res*. 2012;95:2–7.
2. Maurice DM. The location of the fluid pump in the cornea. *J Physiol*. 1972;221:43–54.
3. Engelmann K, Bednarz J, Valtink M. Prospects for endothelial transplantation. *Exp Eye Res*. 2004;78:573–578.
4. Tan DT, Dart JK, Holland EJ, Kinoshita S. Corneal transplantation. *Lancet*. 2012;379:1749–1761.
5. Ang M, Soh Y, Htoon HM, Mehta JS, Tan D. Five-year graft survival comparing descemet stripping automated endothelial keratoplasty and penetrating keratoplasty. *Ophthalmology*. 2016;123:1646–1652.
6. Ang M, Wilkins MR, Mehta JS, Tan D. Descemet membrane endothelial keratoplasty. *Br J Ophthalmol*. 2016;100:15–21.
7. Borkar DS, Veldman P, Colby KA. Treatment of Fuchs endothelial dystrophy by Descemet stripping without endothelial keratoplasty. *Cornea*. 2016;35:1267–1273.
8. Davies E, Jurkunas U, Pineda R II. Predictive factors for corneal clearance after descemetorhexis without endothelial keratoplasty. *Cornea*. 2018;37:137–140.
9. Dirisamer M, Ham L, Dapena I, van Dijk K, Melles GR. Descemet membrane endothelial transfer: "free-floating" donor Descemet implantation as a potential alternative to "keratoplasty". *Cornea*. 2012;31:194–197.
10. Bhogal M, Lwin CN, Seah XY, Peh G, Mehta JS. Allogeneic Descemet's membrane transplantation enhances corneal endothelial monolayer formation and restores functional integrity following Descemet's stripping. *Invest Ophthalmol Vis Sci*. 2017;58:4249–4260.
11. Soh YQ, Mehta JS. Regenerative therapy for Fuchs endothelial corneal dystrophy. *Cornea*. 2018;37:523–527.
12. Soh YQ, Peh GS, Mehta JS. Evolving therapies for Fuchs' endothelial dystrophy. *Regen Med*. 2018;13:97–115.
13. Lovatt M, Yam GH, Peh GS, et al. Directed differentiation of periocular mesenchyme from human embryonic stem cells. *Differentiation*. 2018;99:62–69.
14. Katikireddy KR, Schmedt T, Price MO, Price FW, Jurkunas UV. Existence of neural crest-derived progenitor cells in normal and Fuchs endothelial dystrophy corneal endothelium. *Am J Pathol*. 2016;186:2736–2750.
15. Shaw EL, Rao GN, Arthur EJ, Aquavella JV. The functional reserve of corneal endothelium. *Ophthalmology*. 1978;85:640–649.

16. Dirisamer M, Yeh RY, van Dijk K, et al. Recipient endothelium may relate to corneal clearance in descemet membrane endothelial transfer. *Am J Ophthalmol*. 2012;154:290–296 e291.
17. Arbelaez JG, Price MO, Price FW Jr. Long-term follow-up and complications of stripping descemet membrane without placement of graft in eyes with Fuchs endothelial dystrophy. *Cornea*. 2014; 33:1295–1299.
18. Okumura N, Kinoshita S, Koizumi N. Application of rho kinase inhibitors for the treatment of corneal endothelial diseases. *J Ophthalmol*. 2017; 2017:2646904.
19. Okumura N, Koizumi N, Ueno M, et al. ROCK inhibitor converts corneal endothelial cells into a phenotype capable of regenerating in vivo endothelial tissue. *Am J Pathol*. 2012;181:268–277.
20. Okumura N, Sakamoto Y, Fujii K, et al. Rho kinase inhibitor enables cell-based therapy for corneal endothelial dysfunction. *Sci Rep*. 2016;6: 26113.
21. Okumura N, Matsumoto D, Fukui Y, et al. Feasibility of cell-based therapy combined with descemetorhexis for treating Fuchs endothelial corneal dystrophy in rabbit model. *PLoS One*. 2018;13:e0191306.
22. Breazzano MP, Fikhman M, Abraham JL, Barker-Griffith AE. Analysis of Schwalbe's line (limbal smooth zone) by scanning electron microscopy and optical coherence tomography in human eye bank eyes. *J Ophthalmic Vis Res*. 2013;8:9–16.
23. He Z, Campolmi N, Gain P, et al. Revisited microanatomy of the corneal endothelial periphery: new evidence for continuous centripetal migration of endothelial cells in humans. *Stem Cells*. 2012;30:2523–2534.
24. Yu WY, Grierson I, Sheridan C, Lo AC, Wong DS. Bovine posterior limbus: an evaluation of an alternative source for corneal endothelial and trabecular meshwork stem/progenitor cells. *Stem Cells Dev*. 2015;24:624–639.
25. McGowan SL, Edelhauser HF, Pfister RR, Whikehart DR. Stem cell markers in the human posterior limbus and corneal endothelium of unwounded and wounded corneas. *Mol Vis*. 2007;13:1984–2000.
26. Ang M, Chong W, Huang H, et al. Determinants of posterior corneal biometric measurements in a multi-ethnic Asian population. *PLoS One*. 2014; 9:e101483.
27. Tun TA, Baskaran M, Zheng C, et al. Assessment of trabecular meshwork width using swept source optical coherence tomography. *Graefes Arch Clin Exp Ophthalmol*. 2013;251:1587–1592.
28. Akil H, Huang P, Chopra V, Francis B. Assessment of anterior segment measurements with swept source optical coherence tomography before and after ab interno trabeculotomy (trabectome) surgery. *J Ophthalmol*. 2016;2016: 4861837.
29. Tan GS, He M, Tan DT, Mehta JS. Correlation of anterior segment optical coherence tomography measurements with graft trephine diameter following descemet stripping automated endothelial keratoplasty. *BMC Med Imaging*. 2012;12:19.
30. Yuen LH, He M, Aung T, et al. Biometry of the cornea and anterior chamber in chinese eyes: an anterior segment optical coherence tomography study. *Invest Ophthalmol Vis Sci*. 2010;51:3433–3440.
31. Masis M, Chen R, Porco T, Lin SC. Trabecular meshwork height in primary open-angle glaucoma versus primary angle-closure glaucoma. *Am J Ophthalmol*. 2017;183:42–47.
32. Chen RI, Barbosa DT, Hsu CH, Porco TC, Lin SC. Ethnic differences in trabecular meshwork height by optical coherence tomography. *JAMA Ophthalmol*. 2015;133:437–441.
33. Peh GSL, Ang HP, Lwin CN, et al. Regulatory compliant tissue-engineered human corneal endothelial grafts restore corneal function of rabbits with bullous keratopathy. *Sci Rep*. 2017;7:14149.
34. Khng C, Osher RH. Evaluation of the relationship between corneal diameter and lens diameter. *J Cataract Refract Surg*. 2008;34:475–479.
35. Wang D, Qi M, He M, Wu L, Lin S. Ethnic difference of the anterior chamber area and volume and its association with angle width. *Invest Ophthalmol Vis Sci*. 2012;53:3139–3144.
36. Soh YQ, Peh GS, Mehta JS. Translational issues for human corneal endothelial tissue engineering. *J Tissue Eng Regen Med*. 2017;11:2425–2442.
37. Bostan C, Theriault M, Forget KJ, et al. In vivo functionality of a corneal endothelium transplanted by cell-injection therapy in a feline model. *Invest Ophthalmol Vis Sci*. 2016;57:1620–1634.
38. O'Neal MR, Polse KA. Decreased endothelial pump function with aging. *Invest Ophthalmol Vis Sci*. 1986;27:457–463.
39. Spencer WH, Alvarado J, Hayes TL. Scanning electron microscopy of human ocular tissues: trabecular meshwork. *Invest Ophthalmol* 1968;7: 651–662.
40. Cheung CY, Zheng C, Ho CL, et al. Novel anterior-chamber angle measurements by high-definition optical coherence tomography using

the Schwalbe line as the landmark. *Br J Ophthalmol*. 2011;95:955–959.
41. Wiley L, SundarRaj N, Sun TT, Thoft RA. Regional heterogeneity in human corneal and limbal epithelia: an immunohistochemical evaluation. *Invest Ophthalmol Vis Sci*. 1991;32:594–602.
42. Chee KY, Kicic A, Wiffen SJ. Limbal stem cells: the search for a marker. *Clin Exp Ophthalmol*. 2006;34:64–73.
43. Rachmiel R, Trope GE, Buys YM, Flanagan JG, Chipman ML. Intermediate-term outcome and success of superior versus inferior Ahmed Glaucoma Valve implantation. *J Glaucoma*. 2008;17:584–590.
44. Perez-Torregrosa VT, Olate-Perez A, Cerda-Ibanez M, et al. Combined phacoemulsification and XEN45 surgery from a temporal approach and 2 incisions. *Arch Soc Esp Oftalmol*. 2016;91:415–421.
45. Zhang Y, Huang T, Jorgens DM, et al. Quantitating morphological changes in biological samples during scanning electron microscopy sample preparation with correlative super-resolution microscopy. *PLoS One*. 2017;12:e0176839.
46. Ang M, Konstantopoulos A, Goh G, et al. Evaluation of a micro-optical coherence tomography for the corneal endothelium in an animal model. *Sci Rep*. 2016;6:29769.
47. Tanaka H, Okumura N, Koizumi N, et al. Panoramic view of human corneal endothelial cell layer observed by a prototype slit-scanning wide-field contact specular microscope. *Br J Ophthalmol*. 2017;101:655–659.
48. Okumura N, Matsumoto D, Okazaki Y, et al. Wide-field contact specular microscopy analysis of corneal endothelium post trabeculectomy. *Graefes Arch Clin Exp Ophthalmol*. 2018;256:751–757.